

1 *Research article:*

2 **Epigenetic Malleability at Core Promoter Regulates Tobacco PR-1a**
3 **Expression after Salicylic Acid Treatment**

4
5 **Authors:** Niraj Lodhi^{1*}, Mala Singh¹, Rakesh Srivastava¹, Samir V. Sawant¹, and Rakesh
6 Tuli^{1,3}

7
8 1. National Botanical Research Institute, Council of Scientific and Industrial Research, Rana
9 Pratap Marg, Lucknow-226001, India

10 2. Present address: University Institute of Engineering & Technology (UIET), Sector 25,
11 Panjab University, Chandigarh 160014, India

12

13

14 ***Corresponding Author:**

15 Niraj Lodhi, Ph.D.
16 Lead, Clinical Research (Research and Development Division)
17 Genesis Diagnostics
18 Langhorne, PA 19047
19 Ph: 267-212-2000 Ext. 156
20 Fax: 267-212-2005
21 E-mail: lodhiniraj@gmail.com

22

23

24

25 **SUMMARY**

26 Histone methylation and acetylation regulation of tobacco *PR-1a* promoter are significant for
27 disassembly of the nucleosome and repressor proteins during induction.

28

29 **ABSTRACT**

- 30 • Tobacco's *PR-1a* gene is induced by pathogen attack or exogenous application of
31 Salicylic Acid (SA). However, the epigenetic modifications of the most important
32 inducible promoter of the *PR-1a* gene are not understood clearly.
- 33 • Nucleosome mapping and chromatin immunoprecipitation assay were used to define the
34 histone modification on the *PR-1a* promoter.
- 35 • Here, we report the epigenetic modifications over core promoter lead to disassembly of
36 nucleosome (spans from -102 to +55 bp, masks TATA and transcription initiation) and
37 repressor complex in induced state. ChIP assays demonstrate repressive chromatin of di-
38 methylation at H3K9 and H4K20 of core promoter maintain uninduced state. While,
39 active chromatin marks di and trimethylation of H3K4, acetylation of H3K9 and H4K16
40 are increased and lead the induction of *PR-1a* following SA treatment. TSA enhances
41 expression of *PR-1a* by facilitating the histone acetylation, however increased expression
42 of negative regulator (*SNII*) of *AtPR1*, suppresses its expression in *Arabidopsis thaliana*'s
43 mutants.
- 44 • Constitutive expression of *AtPR1* in Histone Acetyl Transferases (HATs), LSD1, and
45 SNII suggests that its inactive state is indeed maintained by a repressive complex and this
46 strict regulation of pathogenesis related genes is conserved across species.

47

48 **KEYWORDS**

49 Transcription, *PR-1a*, Epigenetics, Histone modifications, Nucleosome, LSD1, Salicylic
50 Acid, Trichostatin A

51

52 INTRODUCTION

53 *PR-1a* (pathogenesis-related-1a) gene is a major defense-related gene of the *PR*
54 family of tobacco (*Nicotiana tabacum*). Linker scanning mutagenesis of the *PR-1a* promoter
55 identified two *as-1* elements and one W-box in the activator region as strong positive, weak
56 negative and strong negative *cis*-elements respectively (Lebel et al., 1998). The core
57 promoter region of the *PR* gene family has a conserved TATA, initiator (INR), and DPE like
58 elements (Lodhi et al., 2008). The detailed chromatin modifications of *PR* gene promoter
59 especially in core promoter sequences during the induction has not been reported yet. Histone
60 modifications dynamically regulate chromatin structure and gene expression for example
61 amino-termini of histones are targets for a series of post-translational modifications including
62 acetylation, methylation, phosphorylation, and ubiquitination (Jenuwein and Allis, 2001;
63 Srivastava and Ahn, 2015; Srivastava et al., 2016; Turner, 2000). Such modifications have
64 been proposed to serve as a ‘histone code’, specifying a chromatin state that determines the
65 transcriptional activity of the genes. Acetylation of histones H3 and H4 is mostly associated
66 with transcriptionally active euchromatin, while methylation is associated with either active
67 or inactive chromatin depending on the methylated amino acid residue (Srivastava et al.,
68 2016; Struhl, 1998), Methylation at H3K4, H3K36, and H3K79 is the hallmark of active
69 transcription, whereas methylation at H3K9, H3K27, and H4K20 is associated with
70 transcriptionally inert heterochromatin (Fischle et al., 2003; Metzger et al., 2005). Lysine can
71 be monomethylated, dimethylated, or trimethylated and each methylation state may have a
72 unique biological function, further increasing the complexity of the ‘histone code’.

73 In higher plants, dynamic regulation of gene expression by histone methylation and
74 acetylation is still not well understood. One of them, a major study of vernalization in
75 *Arabidopsis thaliana* alters the levels of H3 acetylation and H3K9 and H3K27 methylation in
76 a flowering repressor gene (*FLC*) (Bastow et al., 2004; Sung and Amasino, 2004). Histone
77 acetylation is involved in the regulation of the pea plastocyanin gene (Chua et al., 2003; Sung
78 and Amasino, 2004). Dynamic and reversible changes have also been reported in histone
79 H3K4 methylation and H3 acetylation of rice submergence inducible alcohol dehydrogenase
80 I and pyruvate decarboxylase1 genes in response to the presence or absence of stress, (2006).
81 Unlike reversible histone acetylation process, histone methylation was earlier considered as
82 an irreversible modification. However, Ahmad and Henikoff, (2002) identified a process that
83 removes stable histone methylation through histone exchange. Later, histone demethylases

84 such as LSD1 (Chang and Pikaard, 2005; Metzger et al., 2005) and Jumonji C (JmjC domain-
85 containing) protein (Tsukada et al., 2006; Whetstine et al., 2006; Yamane et al., 2006) were
86 also identified. Four LSD1 like proteins have been reported in *A. thaliana* based on conserved
87 domains (amine oxidase and SWIRM) found on the human LSD1 (Chang and Pikaard, 2005).
88 The LSD1 family is conserved from *S. pombe* to humans and regulates histone methylation
89 by both histone methylases and demethylases. Unlike LSD1, which can only remove mono
90 and dimethyl lysine modifications, JmjC-domain-containing histone demethylases (JHDMS)
91 can remove all three histone lysine-methylation states. (Tsukada et al., 2006), (Yamane et al.,
92 2006),

93 Nucleosomes at specific positions serve as general repressors of transcription (Lebel
94 et al., 1998; Srivastava et al., 2014). Repressive nucleosomes are remodeled before
95 (Lomvardas and Thanos, 2002) or concurrently (Benhamed et al., 2006) with transcriptional
96 activation. A nucleosome over the TATA region must be displaced to permit the formation of
97 the pre-initiation complex (Lebel et al., 1998; Srivastava et al., 2014). Our present work
98 analyses the modifications in the chromatin architecture of the core promoter region during
99 *PR-1a* gene induction in response to SA. We showed that the modifications in methylation
100 and acetylation states of histones lead to disassembly of the nucleosome and repressor
101 proteins after SA treatment.

102 MATERIAL AND METHODS

103 Plant materials and growth condition

104 *Nicotiana tabacum* cv. Petite Havana, used as the wild type, was grown in the
105 greenhouse at 22°C±1 in long-day conditions (16 h light–8 h dark). *Arabidopsis thaliana*
106 Col-0 was used as the wild type. All the mutants were in Col-0 background and *Arabidopsis*
107 *LSD1* mutants (Chang and Pikaard, 2005) were obtained from the Arabidopsis Biological
108 Resource Center. *Arabidopsis* plants were grown under controlled environmental conditions
109 (19/21°C, 100 μmol photons m⁻² sec⁻¹, 16 h light/8 h dark cycle). Plant accessions used in the
110 study: X12737, X63603, U66264, AT2G14610, AT4G18470, AT5G54420, AT3G47340,
111 ATU27811.

112 Antibodies used in ChIP experiment

113 Antibodies used in ChIP assay were purchased from Santa Cruz Biotechnology: (anti-
114 acetyl histone H4K16, sc-8662, and anti-acetyl histone H3K9/14, sc-8655), Millipore
115 Corporation (anti-monomethyl histone H3K4 (07-436), anti-dimethyl histone H3K4 (07-030),
116 anti-trimethyl histone H3K4 (07-473), anti-monomethyl histone H3K9 (07-450), anti-
117 dimethyl histone H3K9 (07-441), anti-trimethyl histone H3K9 (07-442), anti-monomethyl
118 histone H4K20(07-440), anti-dimethyl histone H4K20 (07-367), anti-trimethyl histone
119 H4K20 (07-463), and anti-histone H3 (06-755), CoREST, HDAC1 and Arabidopsis anti-
120 LSD1 (developed in our lab).

121 **Plasmid constructions and plant transformation**

122 The *PR-1a* promoter was amplified from the genomic DNA of tobacco by using
123 forward PRF and reverse PRR primers (**Table S1**) and fused to *gusA* gene in pBluescript SK⁺
124 as in Lodhi *et al.*, (2008) (Lodhi et al., 2008). *Agrobacterium tumefaciens* mediated plant
125 transformation was performed comprising construct containing *PR-1a* promoter to examine
126 the expression in stable transgenic lines of *Nicotiana tabacum* cv. Petit Havana.

127 **SA and TSA treatments of plant leaves**

128 The effect of salicylic acid (SA) (Sigma, USA) and Trichostatin A (TSA) (Sigma,
129 USA) on promoter expression were studied on discs. Discs of 3 cm diameter were excised
130 from expanded leaves of transgenic plants and floated on water or 2 mM SA in petri-dish. For
131 inhibition of histone deacetylase, the leaves were treated with 300 μ M TSA. The leaves were
132 incubated for 12 h in light at 25 ± 2 °C. In the case of *A. thaliana*, 100 mg intact 21-days old
133 plantlets were floated on water or SA.

134 **Determination of GUS enzymatic activity**

135 The leaf discs were ground in liquid-nitrogen and extracted with 1 ml GUS assay
136 buffer (50 mM Na₂HPO₄, pH 7, 10 mM EDTA, 0.1% (v/v) Triton X-100, 1 mM DTT, 0.1%
137 (w/v) N-lauryl sarcosine and 25 μ g/ml phenylmethylsulfonyl fluoride . The extract was
138 centrifuged at 16,000 x g for 20 min at 4°C. After centrifugation, 90 μ l supernatant was
139 mixed with 10 μ l GUS assay buffer containing 1 mM of 4-methylumbelliferyl- β -D-
140 glucuronide (MUG) as substrate. The mixture was incubated at 37 °C for 1 h. The product 4-
141 methylumbelliferon (MU) was quantified using a fluorimeter (Perkin Elmer LS55, USA).

142 Protein concentration was determined by Bradford assay (Bio-Rad, Hercules, CA, USA)
143 GUS activity is expressed in units (1 unit = 1 nmol of 4- MU/h/mg of protein).

144 **DNA Sequence mapping of nucleosome's border**

145 The 10 g leaves were treated with water or 2mM SA for 12 h with gentle agitation in
146 light. After 12 h, the samples were subjected to cross-linking in NIB1 buffer (0.5 M hexylene
147 glycol, 20 mM KCl, 20 mM PIPES at pH 6.5, 0.5 mM EDTA, 0.1% Triton X-100, 7 mM 2-
148 mercaptoethanol) in the presence of 1% formaldehyde for 10 min. The cross-linking was
149 stopped by adding glycine to a final concentration of 0.125 M for 5 min at room temperature.
150 The leaves were then rinsed with water, ground to powder in liquid nitrogen, and treated with
151 nuclei isolation buffer NIB1. The extract was filtered through 4 layered muslin cloth and
152 finally filtered sequentially through 80, 60, 40 and 20 μ m mesh sieves. The filtrate was
153 centrifuged at 3,000 x g at 4 °C for 10 min. The pellet was suspended in NIB2 (NIB1 without
154 Triton X-100) and centrifuged again. The pellet was suspended in 5% percoll, loaded on 20-
155 80% percoll (U.S. Biologicals, USA) step gradient and centrifuged. The nuclei were removed
156 from the 20-80% percoll interface, washed in NIB2, and resuspended in NIB1 buffer. The
157 nuclear preparation equivalent to A_{260} of 100 was incubated with micrococcal nuclease (300
158 units/ μ l) (Fermentas, USA) in a buffer containing 25 mM KCl, 4 mM $MgCl_2$, 1 mM $CaCl_2$,
159 50 mM Tris-Cl at pH 7.4 and 12.5% glycerol at 37 °C for 10 min. The reaction was stopped
160 by adding an equal volume of 2% SDS, 0.2 M NaCl, 10 mM EDTA, 10 mM EGTA, 50 mM
161 Tris-Cl at pH 8 and treated with proteinase K (100 μ g/ml) (Ambion, USA) for 1 h at 55 °C.
162 The crosslink was reversed by heating at 65°C overnight. The DNA was extracted by phenol:
163 chloroform and precipitated in ethanol. The DNA was separated on 1.5 % agarose gel and
164 fragments of an average size of 150 bp were purified, denatured, and hybridized with 20 ng
165 of end labeled forward PF3 and reverse NR1 primers of region 1. Primer extension was
166 performed at 37°C using 13 units of sequenase (U.S. Biologicals, USA) in 1x sequenase
167 buffer containing 0.01 M DTT and 0.1 mM dNTPs according to manufacturer's protocol
168 including ladders of all four nucleotides. The products were analyzed in 8% sequencing gels.
169 The sequences of primers used in primer extension are given in **Table S1**.

170 **Detection of nucleosomes on tobacco *PR-1a* promoter using ChIP DNA template**

171 Standard PCR was used to locate nucleosomes in the upstream, downstream, and core
172 promoter regions. MNase digested mononucleosome DNA precipitated with H3 was used as

173 a template to detect the amplicon in uninduced, induced state and TSA treated leaves.
174 Mononucleosomes were purified using Hydroxyapatite (HAP) protocol (Brand et al., 2008).
175 The forward primers (PF3, NPAF1, NPAF5, and NPCF1) and the reverse primers (NR1,
176 NPAR1, NPAR5, and NPCR1) were used to analyze the protection of the core promoter (-
177 102 to +55 bp), the upstream (-362 to -213 and -262 to -102 bp) and downstream (+59 to
178 +208 bp) regions respectively of the *PR-1a* promoter against micrococcal nuclease digestion
179 in the uninduced and induced states. The sequences of all primers are given in **Table S1**. To
180 do native ChIP, 1.5 – 2 g leaf discs of tobacco excised from 8-9 week old plants were floated
181 on water or 2mM SA and 300 μ M TSA for 12 h with gentle agitation in the light. After 12 h
182 the samples were rinsed with water and ground into powder in liquid nitrogen. Nuclei were
183 extracted and washed with 1 ml of buffer N (15 mM Trizma base, 15mM NaCl, 60mM KCl,
184 250mM sucrose, 5mM MgCl₂, 1 mM CaCl₂, pH-7.5, 7 mM 2-mercaptoethanol, 1 mM
185 phenylmethylsulfonyl fluoride, and 50 μ l/ml plant protease inhibitor cocktail) (Sigma
186 chemicals, USA). Thereafter nuclei were suspended in 100 μ L buffer N. DNA content was
187 estimated in a 10 μ l aliquot and MNase treatment were given using 1unit/ μ g DNA for 10 min
188 at 37°C., and finally eluted in 300 μ L of HAP elution buffer (500mM Na₂PO₄ pH7.2,
189 100mMNaCl, 1mM EDTA) and was diluted with 1700 μ L of ChIP dilution buffer (1.1%
190 Triton X-100, 1.2 mM EDTA, 16.7 mM Tris-HCl, pH 8, 167 mM NaCl, and 50 μ l/ml
191 protease inhibitor cocktail). The diluted chromatin solution was then subjected to 1 h of pre-
192 cleaning treatment at 4°C with 80 μ l of salmon sperm DNA/protein agarose (Upstate; 16-
193 157). An aliquot of 50 μ l was removed for the total input DNA control. Immunoprecipitation
194 was performed overnight (18 h) at 4°C using 600 μ L chromatin solution with histone H3
195 antibodies (typically at 1:150 final dilutions) or without antibodies (mock control).
196 Immunoprecipitates were collected after incubation with 40 μ L of salmon sperm
197 DNA/protein agarose (50% suspension in dilution buffer) at 4°C for 1 h. The protein A
198 agarose beads bearing immunoprecipitate were then subjected to sequential washes and
199 eluted twice with 250 μ L elution buffer each time (1% SDS and 0.1M NaHCO₃). For the
200 input DNA control (50 μ L), 450 μ L elution buffer was added. Protein was removed by 1.1 μ L
201 proteinase K (20mg/ml) at 45° C for 1h and RNA by 2 μ L of RNaseA (1mg/ml) digestion at
202 37°C for 1h. The DNA was purified by phenol: chloroform extraction and ethanol
203 precipitation. Purified DNA was resuspended in 50 μ L TE buffer for PCR analysis.

204 **Southern hybridization to detect nucleosomes in promoter region of tobacco *PR-1a***

205 Twenty micrograms of purified MNase-digested DNA was analyzed to find out the
206 position of nucleosomes in *PR-1a* promoter. Eight probes of 200 bp from the core promoter
207 region were designed (R1 to R8). For positive control, 10 pg *PR-1a* promoter (PCR
208 amplified) and for negative control 10 pg of sonicated calf thymus DNA was used. The entire
209 DNA was transferred on to nylon membrane and incubated at 42°C overnight with a probe.

210 **ChIP PCR using precipitated DNA with different antibodies**

211 The leaf discs (1.5 – 2 g) of tobacco excised from 8-9-week-old plants were floated on
212 water or 2mM SA for 12 h with gentle agitation in light. After 12 h the samples were
213 subjected to 1% formaldehyde cross-linking in a cross-link buffer (0.4 M sucrose, 10 mM
214 Tris-HCl, pH 8, and 1 mM EDTA) under vacuum for 10 min. Formaldehyde cross-linking
215 was stopped by adding glycine to a final concentration of 0.125 M and incubating for 5 min
216 at room temperature. The leaf pieces were then rinsed with water and ground to powder in
217 liquid nitrogen. Nuclei were extracted and lysed with 300 µl of lysis buffer (50 mM Tris-HCl,
218 pH 8, 10 mM EDTA, 1% SDS, 1 mM phenylmethylsulfonyl fluoride, 10 mM Sodium
219 butyrate, 1 mM benzamidine, and 50 µL/ml protease inhibitor cocktail) (Sigma chemicals,
220 USA). The resulting chromatin was subjected to pulse sonication (six pulses, 95% power
221 output for eight times) using a Branson M3210 (Danbury, USA) to obtain DNA fragments
222 with size ranging from 500 to 1000 bp. After sonication, a 25 µl aliquot was removed for the
223 total input DNA control, and the rest of the chromatin solution was diluted 10 times with
224 ChIP dilution buffer (1.1% Triton X-100, 1.2 mM EDTA, 16.7 mM Tris-HCl, pH 8, 167 mM
225 NaCl, and 50 µl/ml protease inhibitor cocktail). The diluted chromatin solution was then
226 subjected to 1 h of precleaning treatment at 4°C with 40 µl of salmon sperm DNA/protein
227 agarose (Upstate; 16-157) (50% suspension in dilution buffer without Na butyrate and
228 protease inhibitor cocktail) to reduce nonspecific interactions between protein-DNA
229 complexes and the agarose beads. Immunoprecipitation was performed overnight (18 h) at
230 4°C using 600 µL chromatin solution with antibodies (typically at 1:150 final dilutions) or
231 without antibodies (mock control). Immunoprecipitates were collected after incubation with
232 40 µL of salmon sperm DNA/protein agarose (50% suspension in dilution buffer) at 4°C for 1
233 h. The protein A agarose beads bearing immunoprecipitate were then subjected to sequential
234 washes and eluted twice with 250 µL elution buffer (1% SDS and 0.1M NaHCO₃). Samples
235 were then reverse cross-linked at 65°C under high salt (0.2 M NaCl) for 6 h. For the input
236 DNA control (25 µL), 275 µL TE buffer (10 mM Tris-HCl, pH 8, and 1 mM EDTA) was

237 added and reverse cross-linked. After reversing the cross-links, the protein was removed by
238 1.1 μ L of proteinase K (20mg/ml) at 45° C for 1h and RNA by 2 μ L of RNaseA (1mg/ml)
239 (Qiagen) digestion at 37°C for 1h. The DNA was purified by phenol: chloroform extraction
240 and ethanol precipitation. Purified DNA was resuspended in 40 μ L TE buffer for PCR
241 analysis.

242 For ChIP PCR the target region of the *PR-1a* promoter was -102 to +55 with
243 reference to the transcription start site. Forward primer PF3 and reverse primer NR1 were
244 used for amplifying the core promoter. Tobacco *ACTIN* promoter was taken as an internal
245 control for active chromatin, using forward AGF and reverse AGR primers for PCR **Table**
246 **S1**. For testing the enrichment of various modifications on the R8 promoter at different time
247 points, forward primer PF3 and reverse primer NR1 were used for qRT-PCR. Reactions were
248 placed in 25 μ l volume in triplicate according to the manufacturer's instruction (Invitrogen
249 SYBR green ER) on ABI PRISM 7500.

250 **Transcripts detection of different defense related genes of *Arabidopsis* using** 251 **Quantitative real-time PCR**

252 To compare the transcript levels of *AtPRI*, *AtSNII*, *AtPDF1.2*, and *AtASNI*, leaves of
253 wild type *A. thaliana* plants (Col-0) were treated with water, 2 mM SA, TSA alone or TSA
254 and SA both. After 12 h, total RNA isolated by Tri-reagent (Sigma) and treated with RNase
255 free DNase. For temporal expression of tobacco *PR-1a*, the total RNA was isolated from the
256 leaf discs which were floated on SA for different time periods. The first strand cDNA was
257 synthesized, using 2 μ g RNA, as per manufacturer's instructions (Invitrogen, USA).
258 Quantitative real-time PCR (qRT-PCR) was used to determine the expression of *AtPRI* in
259 uninduced and induced states, using forward ATPRF and reverse ATPRR primers. Tobacco
260 *PR-1a* expression at different time points was followed by standard PCR by using forward
261 NPRF and reverse NPRR primers. The *AtACTIN7* and *UBIQUITIN* genes were used as an
262 internal control. The sequences of primers used are given in **Table S1**.

263 **RESULTS**

264 **Nucleosome over core promoter of *PR-1a* spans from -102 to +55 bp in uninduced state**

265 Earlier, we reported a distinct nucleosome over the core promoter region of *PR-1a* in
266 the uninduced state disassembles upon SA induction to initiate the transcription (Lodhi et al.,

267 2008). In the present study, we reported mapping of nucleosome using a primer extension
268 method. It was performed after confirming the presence of nucleosome as well as on entire
269 promoter of *PR-1a* by southern hybridization. We performed by deviding the entire length of
270 the *PR-1a* promoter (1.5Kb) into eight distinct regions of around 200 bp (R1 to R8). The
271 region encompassing the core promoter and transcription start site (TSS) was designated as
272 R8 (Fig. S1). The mono-nucleosome template from uninduced tobacco plants was prepared
273 by digesting with micrococcal nuclease (MNase) enzyme (digest the linker region). Probes
274 from different regions of the *PR-1a* promoter were used in southern hybridization with the
275 MNase digested mono-nucleosome template. Southern hybridization reveals the presence of
276 nucleosomes over five regions including R1, R2, R4, R5 and R8 on promoter (Fig. S1).
277 Nucleosome boundaries of R8 nucleosome (over core promoter) were mapped using the
278 primer extension method with forward (PF3) and reverse (NR1) primers (Fig. 1A is showing
279 the sequencing with one primer). The boundaries of the nucleosome were found to be
280 spanning from -102 to +55 bp (with respect to the TSS) in *PR-1a* (Fig. 1B). The nucleosome
281 over R8 masked the TATA region, transcription initiation site (+1), and downstream
282 promoter region (-102 to +55 bp) in the uninduced state of *PR-1a*.

283 **Histone acetylation (H3K9Ac and H4K16Ac) marks associated with the activation of** 284 ***PR-1a* followed by SA treatment**

285 It was demonstrated that the *PR-1a* induction coincided with the disappearing or
286 disassembly of the nucleosome over region 8 (R8) (Lodhi et al., 2008). Here, we further
287 examined the epigenetic changes in chromatin responsible for the disassembly of the
288 nucleosome. Since histone acetylation associated with transcriptional activation and histone
289 acetylation of H3K9/14 and H4K16 has been demonstrated in the activation of genes (Santos-
290 Rosa and Caldas, 2005; Shahbazian and Grunstein, 2007; Shogren-Knaak and Peterson,
291 2006). We checked the acetylation status of the H3K9 and H4K16 of R8 nucleosome using
292 the ChIP approach in a time-dependent manner. ChIP results showed that the onset of
293 transcription of *PR-1a* strongly correlated with the H3K9/14 and H4K16 acetylation.
294 Acetylation of these lysine residues increased gradually from 3 to 9h post-SA treatment
295 reaching maximum at 9h (Fig. 2A and B).

296 To examine whether *PR1* locus genetically interacted with histone acetyltransferases,
297 we performed experiments in *Arabidopsis thaliana* (Ws) because histone acetyltransferase
298 mutants' plants of tobacco were not available and also assuming histone acetyltransferases

299 are conserved across the plant species. Three HAT mutants of *Arabidopsis thaliana* (Ws) i.e.
300 HAG3, HAC1, and HXA1 were examined. The estimation of *AtPR1* transcript in the mutants
301 in uninduced states showed a significant increase of transcript as compared to the wild type.
302 An increase in the uninduced expression of *AtPR1* suggested the loss of stringent regulation
303 of *PR1* in the uninduced condition (Fig. 2C). Therefore, histone acetyltransferases HAG3,
304 HAC1, and HXA1 are essential to acetylate histone marks of nucleosome to activate the
305 transcription of *AtPR1*.

306 **Nucleosome disassembly of *PR-1a* core promoter is required for transcriptional** 307 **activation**

308 The disappearance of the nucleosome could be either due to nucleosome sliding or
309 complete disassembly. To further understand the fate of nucleosome remodeling at the *PR-1a*
310 core promoter, we addressed the histone H3 occupancy either on Group 3 (R8) or on flanking
311 upstream Group 1 or 2 and downstream promoter region group 4 of *PR-1a* by ChIP using
312 anti-H3 antibody in uninduced and SA treated leaves. We observed distinct nucleosome over
313 group 3 (R8, -102 to +55) as evident PCR amplified product in case of uninduced control
314 (Fig. 1). Since SA treatment affects histone acetylation of the nucleosome over *PR-1a* core
315 promoter region upon the induction (Fig. 2), the histone H3 occupancy was also studied in
316 Trichostatin A (TSA, an inhibitor of histone deacetylase) treated tobacco leaf discs in the
317 presence or absence of SA (Fig. 3). The nucleosome over group 3 disappeared with SA
318 induction, however treatment with TSA in the presence or absence of SA inhibited
319 nucleosome disappearance (Fig. 3A). We did not observe nucleosome protection over group
320 2 (-213 to -102) in any of the conditions tested indicating the lack of nucleosome over this
321 region (Fig. 3B).

322 Multiple sets of primer pairs and ChIP template DNA were used to detect
323 nucleosomes associated with different regions of the core promoter and flanking promoter of
324 *PR-1a* (Fig. 4). Therefore, results suggest a explanation for the repression of *AtPR1* transcript
325 with TSA treatment in *A. thaliana* (discussed later). The promoter flanking region in group 1
326 (-362 to -213) and group 4 (+59 to +208) also have distinct nucleosomes, however, these
327 nucleosomes did not show any change post-SA or TSA treatment.

328 **Temporal regulation of *PR-1a* by SA treatment correlates with the acetylation of H3-** 329 **K9/14 of core promoter nucleosome**

330 The *PR-1a* is a late inducible promoter, its activation was noticed 9 h after SA
331 treatment (Fig. 4). To further understand the correlation between *PR-1a* transcription and
332 acetylation of its promoter, we studied the temporal regulation of *PR-1a* in response to SA
333 and performed ChIP with acetylated H3K9/14 and tri-methylated H3K4 antibodies on the
334 core promoter at different time points. The onset of transcription of *PR-1a* was correlated
335 strongly with the acetylation of H3K9/14 (Fig. 4). The H3K9/14 was highly acetylated at 9 h,
336 remained so till 12 h post-SA treatment, and then declined. The results indicated that during 9
337 to 12 h post-SA treatment, there was a sharp, though the transient increase in acetylation of
338 H3 in the nucleosome of the core promoter, whereas a slight increase in tri-methylation of
339 H3K4 from 6 to 9 h post-SA treatment.

340 **TSA enhances early expression of tobacco *PR-1a* followed by SA treatment**

341 The effect of HDAC inhibitor TSA was examined on the expression of *PR-1a*. The
342 leaves were treated with SA for 4h (to get the induction signal) and then shifted to either
343 water or TSA. The expression of *PR-1a* promoter was examined by assaying the *GUS*
344 reporter gene fused to it. The analysis of three independent transgenic lines showed a clear
345 effect of TSA. The expression was higher in the TSA treated leaves till 25 h in comparison to
346 the water treated leaves (Fig. 5). Higher expression correlated well with the H3K9/14
347 acetylation (Fig. 4). After 25 h, there was no difference in expression in the two cases. The
348 results indicated that short exposure to SA leads to transcription of *PR-1a* which was
349 vulnerable to suppression by HDACs. However, after 25 h in water or TSA, stable H3K9/14
350 acetylation- insensitive expression was noticed.

351 **Histone methylation plays a dual role in the transcriptional regulation of *PR-1a***

352 The role of histone methylation of nucleosome over the core promoter in *PR-1a*
353 expression was also examined, using ChIP-qRT-PCR with antibodies specific to mono-, di-
354 or tri- methylated H3K4, H3K9 and H4K20. A gradual increase in H3K4 me2 (Fig. 6A),
355 H3K4me3 (Fig. 6B) and H3K9 me3 (Fig. 6F) was observed till 9h post-SA treatment
356 coinciding with transcription activation of *PR-1a* (Fig. 4) and removal of nucleosome from
357 the core promoter (Fig. 3). In contrast, H3K9 me1 (Fig. 6D) and me2 (Fig. 6E) were found to
358 be enriched in the uninduced conditions and decreased subsequently post the SA treatment.
359 H3K4 mono-methylation increased gradually up to 9h accompanies the transcriptional
360 activation at 9h post-SA treatment (Fig. 6A). An increased trimethylation of lysine residues

361 of H3K9 showed a dual role of histone methylation (activation and repression) in the
362 transcriptional regulation of *PR-1a*. The methylation state of H4K20 was studied further,
363 mono-, di- and tri- methylation of H4K20 (Fig. 6G-I) showed significantly low signals.

364 **The Human Lysine Specific Demethylase 1 (LSD1) like gene maintains silent state of** 365 ***PR-1a* in uninduced state**

366 To examine whether *PR1* locus genetically interacted with LSD1 like genes, we
367 performed experiments in *Arabidopsis thaliana* (Ws) because LSD1 like mutants of tobacco
368 plant were not available. Four putative homologs (1 to 4) of LSD1 have been reported in *A.*
369 *thaliana* viz. At3G13682, At3G10390, At1G62830 and At4G16310 (Chang and Pikaard,
370 2005). We carried out quantitative real-time PCR of *AtPR1* transcript in these *lsd1* like
371 mutants in the uninduced state. In all the four mutants, a high level of *AtPR1* was noticed in
372 the uninduced state in contrast to a very low level of uninduced *AtPR1* in wild type (Fig. 7A).
373 The mutations in LSD1 like genes (At3G10390, At1G62830, and At4G16310) led to nearly
374 constitutive expression of *AtPR1*. The results established that the lysine-specific demethylase
375 family was involved in giving repressed chromatin conformation to the *AtPR1* region in *A.*
376 *thaliana* in the uninduced state. The results on *lsd1* mutants encouraged us to determine the
377 recruitment of LSD1 on the core promoter region of *PR-1a*.

378 **TSA enhances the expression of *AtSNII*, a negative regulator of *AtPR1***

379 Tobacco *PR-1a* promoter was not induced in the presence of TSA alone. To address
380 why TSA prevents the induction of *PR-1a*, we carried out experiments on *Arabidopsis*
381 *thaliana* (Columbia ecotype) because the regulators of *PR-1a* gene in tobacco have not been
382 identified. In *A. thaliana*, a negative regulator gene of *AtPR1*, called *AtSNII* has earlier been
383 reported (Mosher et al., 2006). The expression of the regulatory genes was examined after
384 treatment with SA and TSA. The *AtSNII* gene was not activated by SA treatment but was
385 induced by TSA (Fig. 7B). The jasmonic acid (JA) inducible *AtPDF1.2* gene was repressed
386 by SA (Spoel et al., 2003), while TSA did not affect its expression. The TSA inducible
387 *AtGDAS* was used as a positive control and *AtACTIN7* as an internal control in the
388 experiments.

389 **LSD1-CoREST-HDAC1 complex maintains the silent state of *PR-1a***

390 Our results suggest the LSD1 maintains the silent state of *PR-1a* in the uninduced
391 condition. In other studies, LSD1 was reported to be a part of the LSD1-CoREST-HDAC1
392 suppressor complex of neuronal genes in non-neural cells (Ballas et al., 2001). We examined
393 whether this repressor complex was involved in maintaining the silent state of *PR-1a* also in
394 the uninduced state. First, we checked the presence of LSD1 like protein on the core
395 promoter region in uninduced state. ChIP analysis of *PR-1a* locus was carried out in
396 uninduced and induced states using custom made (Supplementary information 5) anti-LSD1
397 specific antibody. ChIP qRT-PCR result suggested that LSD1 like protein was indeed present
398 on the core promoter region in the uninduced state (Fig. 8A). Next, we looked for the LSD1-
399 CoREST-HDAC1 Complex on *PR-1a* locus. We performed ChIP using again anti-LSD1 like,
400 anti-CoREST and anti-HDAC1 specific antibodies. The results indicate the presence of
401 CoREST and HDAC1 in the uninduced state of *PR-1a* chromatin similar as noticed for
402 LSD1. The CoREST and HDAC1 were reduced when *PR-1a* was activated by SA (Fig. 8B).

403 **DISCUSSION**

404 Salicylic acid (SA) is the key signal molecule for the establishment of systemic
405 acquired resistance (SAR). Transcripts of tobacco *PR-1a* or *AtPRI* is accumulated in
406 response to SA signalling, which is a marker for the establishment of SAR (Loake and Grant,
407 2007; Vlot et al., 2009). Several efforts were made to elucidate the molecular mechanism of
408 transcriptional regulation of *PR* genes (Kesarwani et al., 2007; Wang et al., 2009). In our
409 present study, we focused on the epigenetic regulation core promoter nucleosome of the *PR-1a*
410 gene and identified five nucleosomes over the promoter region of *PR-1a* in the uninduced
411 condition spanning from the TATA-box and transcription initiation site to upstream region
412 (as-1 like element) (Fig. 1A and B; Fig. 1S B). The nucleosome over the TATA-box is
413 responsible for the silent state of *PR-1a* transcription in the uninduced condition (Lodhi et al.,
414 2008) and the unmasking of the TATA-box region is crucial to establish the pre-initiation
415 complex and recruitment of RNA polymerase II (Cairns, 2009; Juven-Gershon and
416 Kadonaga, 2009; Kiran et al., 2006). The mechanism involving masking of the TATA-box by
417 the nucleosome and suppression of transcription has been reported in several eukaryotic
418 promoters (Lebel et al., 1998; Srivastava et al., 2014; Workman and Kingston, 1998). The
419 nucleosome over the region 8 (R8) (Fig. 1S B) disappears post-SA treatment (Fig. 3; group 3
420 (R8)) and coincides with the *PR-1a* transcription (Fig. 4). The disappearance of the
421 nucleosome over the R8 could be either because of nucleosome sliding (Lomvardas and

422 Thanos, 2001) or nucleosome disassembly (Adkins et al., 2007; Boeger et al., 2004) both the
423 mechanisms have been demonstrated in detail in different eukaryotic promoters (Boeger et
424 al., 2005). Our native ChIP experiment using anti-H3 antibody (Fig. 2 A and B) establishes
425 that the disappearance of the nucleosome over the R8 (group 3) could not be possible because
426 of sliding since the region immediately downstream of the core promoter (group 4) was
427 occupied by a nucleosome and region immediately upstream (group 2) is always free of the
428 nucleosome. It further confirms the lack of core histone from the R8 (group 3) in the SA
429 induced condition (Fig. 3). Thus, our results strongly support that the disappearance of the
430 nucleosome over the R8 post-SA treatment is due to complete nucleosome disassembly. The
431 *Anti-Silencing Function1* gene (*Asf1*) is reported to disassemble the nucleosome in budding
432 yeast (Adkins et al., 2007). Homologs of *Asf1* have been reported from *A. thaliana* as well,
433 suggested the possibility that nucleosome over the core region of tobacco *PR-1a* is
434 disassembled by homologues of such genes.

435 Following SA induction of *PR-1a*, acetylation of H3K9/14 increased 9 h post-SA
436 treatment (Fig. 2 A and B), similar to transgenic plants with *PR-1a*:GUS, the expression of
437 GUS protein was detected at 10 h post SA induction (Fig. 5) (Lodhi et al., 2008). A rapid
438 transient increase in acetylation of H3K9/14 at 9 h and a slight increase in tri-methylation of
439 H3K4 in the activation of *PR-1a* transcription at the same time (Fig. 4) indicate that the H3-
440 K9/K14 acetylation is required for the active state of *PR-1a* core promoter. The acetylation of
441 H3-K9/14 has been reported in the activation of *RBCS-1A* and *IAA3* genes (Benhamed et al.,
442 2006). Microarray analyses in tobacco and *A. thaliana* seedlings show that TSA induces
443 changes in gene expression and affects histone acetylation in specific genes (Chang and
444 Pikaard, 2005; Chua et al., 2004). In *A. thaliana*, histone deacetylase *AtHDI* (also called
445 HDA19) is involved in the regulation of pathogen response genes (Zhou et al., 2005). We
446 observed TSA mediated suppression of *AtPRI* transcription (Fig. 7B) and also inhibition in
447 nucleosome modeling at the core promoter (Fig. 3) when TSA was provided along with SA.
448 These results were surprising in the context of the importance of H3K9/14 and H4K16
449 acetylation required for *PR-1a* activation (Fig. 2A-B). One possible explanation could be that
450 TSA mediated suppression of *PR-1a* is indirect by higher expression of a negative regulator
451 of *PR-1a* locus.

452 Modification of the histone H3K4 di- and tri-methylation also enrich till 9h post-
453 induction and positively correlate transcriptional activation (Fig. 6B-C). Mono methylation of

454 H3K4 is initially very little enrichment and its transient mild enrichment till 9h at the *PR-Ia*
455 promoter. Earlier reports also suggest that the presence of H3K4me2 and H3K4me3 in plants
456 is usually correlated with the active transcription of the highly expressed genes, whereas
457 H3K4me1 is distributed within transcribed regions (Zhang et al., 2009). Our results also
458 suggested that histone modification such as mono and dimethylation at lysine 9 and 20 of H3
459 and H4 respectively were found increased in the uninduced state of *PR-Ia* (Fig. 6D, E, and
460 H). This agrees with the earlier reports that H4K20 methylation results in the repression of
461 genes, which is associated with silent chromatin and inhibits acetylation of H4K16
462 (Karachentsev et al., 2005; Sarg et al., 2004; Sims et al., 2003). Following SA induction, a
463 decrease in H3K9 mono- and di-methylation suggested their involvement in repressing the
464 locus in the uninduced state, also reported by several other studies (Bernatavichute et al.,
465 2008; Fuchs et al., 2006; Jackson et al., 2004; Johnson et al., 2004; Lippman et al., 2004;
466 Mathieu et al., 2005). This decrease may be their conversion to the trimethylated state as
467 shown by the H3K9 trimethylation enrichment, which is a mark for transcriptional activation
468 (Turck et al., 2007). Lack of H4K20 methylation in transcriptionally active regions has also
469 been reported in the *Drosophila* male X chromosome as the methylation of H4K20 precludes
470 acetylation of the neighboring H4K16, both processes being competitive (Nishioka et al.,
471 2002). However, ORC1-dependent gene activation in plants is associated with an increase in
472 H4 acetylation and H4K20 trimethylation (de la Paz Sanchez and Gutierrez, 2009).
473 Moreover, monomethylated H4K20 is associated with heterochromatin, and di- and tri-
474 methylated H4K20 are associated with euchromatin in *Arabidopsis* (Naumann et al., 2005).

475 It is conceivable that the loss in di- and tri-methylation of H4K20 and di-methylation
476 of H3K4 in *PR-Ia* in the induced state results from enzymatic demethylation. A human LSD1
477 that demethylates mono and di-methylated H3K4 has been identified (Chang and Pikaard,
478 2005), suggesting involvement of LSD1 like genes in tobacco for demethylation of the di-
479 methylated H3K4. Full enzymatic activity of LSD1 requires its association with other
480 proteins, such as CoREST (restin corepressor) complex, indicating that regulatory subunits
481 can have a role in modulating demethylase activity (Chang and Pikaard, 2005; Lee et al.,
482 2005). The presence of a nucleosome over the core promoter has often been associated with
483 transcriptional silencing of genes (Lebel et al., 1998; Srivastava et al., 2014). Our study
484 shows that five nucleosomes cover the promoter region of *PR-Ia* including a nucleosome
485 over the downstream region (core promoter) or upstream activator region (covers *as-1*-like
486 element responsible for induction) (Butterbrodt et al., 2006). After induction, the nucleosome

487 over the core promoter disassembles and provides the access to transcription initiation
488 machinery on nucleosome-free core promoter region. In conclusion, we suggest nucleosome
489 association with LSD1-CoREST-HDAC1 suppressor like complex maintain the silent state of
490 *PR-1a* locus (Fig. 8).

491

492 **ACKNOWLEDGMENTS**

493 The authors are grateful to Council of Scientific and Industrial Research (CSIR) for
494 Junior/Senior Research Fellowship to Niraj Lodhi and Department of Sciences and
495 Technology, Government of India for the research grant, J.C. Bose and Research Fellowships
496 to Dr. Rakesh Tuli.

497 **Declaration of competing interest**

498 The authors declare no conflicts of interest

499

500 **SUPPLEMENTARY INFORMATION**

501 **Table S1** List of primers used in this study.

502 **Figure S1** Position of nucleosomes on promoter of PR-1a in uninduced state.

503

504 **REFERENCES**

- 505 Adkins, M.W., Williams, S.K., Linger, J., Tyler, J.K. (2007) Chromatin disassembly from the PHO5
506 promoter is essential for the recruitment of the general transcription machinery and
507 coactivators. *Molecular and Cellular Biology*, **27**(18), 6372-6382.
- 508 Ahmad, K. and Henikoff, S. (2002) The histone variant H3.3 marks active chromatin by replication-
509 independent nucleosome assembly. *Molecular Cell*, **9**(6), 1191-1200.
- 510 Ballas, N., Battaglioli, E., Atouf, F., Andres, M.E., Chenoweth, J., Anderson, M.E., Burger, C.,
511 Moniwa, M., Davie, J.R., Bowers, W.J., Federoff, H.J., Rose, D.W., Rosenfeld, M.G., Brehm,
512 P., Mandel, G. (2001) Regulation of neuronal traits by a novel transcriptional complex.
513 *Neuron*, **31**(3), 353-365.
- 514 Bastow, R., Mylne, J.S., Lister, C., Lippman, Z., Martienssen, R.A., Dean, C. (2004) Vernalization
515 requires epigenetic silencing of FLC by histone methylation. *Nature*, **427**(6970), 164-167.
- 516 Benhamed, M., Bertrand, C., Servet, C., Zhou, D.X. (2006) Arabidopsis GCN5, HD1, and
517 TAF1/HAF2 interact to regulate histone acetylation required for light-responsive gene
518 expression. *The Plant Cell*, **18**(11), 2893-2903.
- 519 Bernatavichute, Y.V., Zhang, X., Cokus, S., Pellegrini, M., Jacobsen, S.E. (2008) Genome-wide
520 association of histone H3 lysine nine methylation with CHG DNA methylation in Arabidopsis
521 thaliana. *PLoS One*, **3**(9), e3156.
- 522 Boeger, H., Bushnell, D.A., Davis, R., Griesenbeck, J., Lorch, Y., Strattan, J.S., Westover, K.D.,
523 Kornberg, R.D. (2005) Structural basis of eukaryotic gene transcription. *FEBS Letters*,
524 **579**(4), 899-903.
- 525 Boeger, H., Griesenbeck, J., Strattan, J.S., Kornberg, R.D. (2004) Removal of promoter nucleosomes
526 by disassembly rather than sliding in vivo. *Molecular Cell*, **14**(5), 667-673.

- 527 Brand, M., Rampalli, S., Chaturvedi, C.P., Dilworth, F.J. (2008) Analysis of epigenetic modifications
528 of chromatin at specific gene loci by native chromatin immunoprecipitation of nucleosomes
529 isolated using hydroxyapatite chromatography. *Nature Protocols*, **3**(3), 398-409.
- 530 Butterbrodt, T., Thurow, C., Gatz, C. (2006) Chromatin immunoprecipitation analysis of the tobacco
531 PR-1a- and the truncated CaMV 35S promoter reveals differences in salicylic acid-dependent
532 TGA factor binding and histone acetylation. *Plant Mol Biol*, **61**(4-5), 665-674.
- 533 Cairns, B.R. (2009) The logic of chromatin architecture and remodelling at promoters. *Nature*,
534 **461**(7261), 193-198.
- 535 Chang, S. and Pikaard, C.S. (2005) Transcript profiling in Arabidopsis reveals complex responses to
536 global inhibition of DNA methylation and histone deacetylation. *Journal of Biological*
537 *Chemistry*, **280**(1), 796-804.
- 538 Chua, Y.L., Mott, E., Brown, A.P., MacLean, D., Gray, J.C. (2004) Microarray analysis of chromatin-
539 immunoprecipitated DNA identifies specific regions of tobacco genes associated with
540 acetylated histones. *The Plant Journal*, **37**(6), 789-800.
- 541 Chua, Y.L., Watson, L.A., Gray, J.C. (2003) The transcriptional enhancer of the pea plastocyanin
542 gene associates with the nuclear matrix and regulates gene expression through histone
543 acetylation. *The Plant Cell*, **15**(6), 1468-1479.
- 544 de la Paz Sanchez, M. and Gutierrez, C. (2009) Arabidopsis ORC1 is a PHD-containing H3K4me3
545 effector that regulates transcription. *Proceedings of the National Academy of Sciences*,
546 **106**(6), 2065-2070.
- 547 Fischle, W., Wang, Y., Allis, C.D. (2003) Histone and chromatin cross-talk. *Current Opinion in Cell*
548 *Biology*, **15**(2), 172-183.
- 549 Fuchs, J., Demidov, D., Houben, A., Schubert, I. (2006) Chromosomal histone modification patterns--
550 from conservation to diversity. *Trends in Plant Science*, **11**(4), 199-208.
- 551 Jackson, J.P., Johnson, L., Jasencakova, Z., Zhang, X., PerezBurgos, L., Singh, P.B., Cheng, X.,
552 Schubert, I., Jenuwein, T., Jacobsen, S.E. (2004) Dimethylation of histone H3 lysine 9 is a
553 critical mark for DNA methylation and gene silencing in Arabidopsis thaliana. *Chromosoma*,
554 **112**(6), 308-315.
- 555 Jenuwein, T. and Allis, C.D. (2001) Translating the histone code. *Science*, **293**(5532), 1074-1080.
- 556 Johnson, L., Mollah, S., Garcia, B.A., Muratore, T.L., Shabanowitz, J., Hunt, D.F., Jacobsen, S.E.
557 (2004) Mass spectrometry analysis of Arabidopsis histone H3 reveals distinct combinations of
558 post-translational modifications. *Nucleic Acids Res*, **32**(22), 6511-6518.
- 559 Juven-Gershon, T. and Kadonaga, J.T. (2009) Regulation of gene expression via the core promoter
560 and the basal transcriptional machinery. *Developmental Biology*, **339**(2), 225-229.
- 561 Karachentsev, D., Sarma, K., Reinberg, D., Steward, R. (2005) PR-Set7-dependent methylation of
562 histone H4 Lys 20 functions in repression of gene expression and is essential for mitosis.
563 *Genes & Development*, **19**(4), 431-435.
- 564 Kesarwani, M., Yoo, J., Dong, X. (2007) Genetic interactions of TGA transcription factors in the
565 regulation of pathogenesis-related genes and disease resistance in Arabidopsis. *Plant*
566 *Physiology*, **144**(1), 336-346.
- 567 Kiran, K., Ansari, S.A., Srivastava, R., Lodhi, N., Chaturvedi, C.P., Sawant, S.V., Tuli, R. (2006) The
568 TATA-box sequence in the basal promoter contributes to determining light-dependent gene
569 expression in plants. *Plant Physiology*, **142**(1), 364-376.
- 570 Lebel, E., Heifetz, P., Thorne, L., Uknes, S., Ryals, J., Ward, E. (1998) Functional analysis of
571 regulatory sequences controlling PR-1 gene expression in Arabidopsis. *The Plant Journal*,
572 **16**(2), 223-233.
- 573 Lee, M.G., Wynder, C., Cooch, N., Shiekhattar, R. (2005) An essential role for CoREST in
574 nucleosomal histone 3 lysine 4 demethylation. *Nature*, **437**(7057), 432-435.
- 575 Lippman, Z., Gendrel, A.V., Black, M., Vaughn, M.W., Dedhia, N., McCombie, W.R., Lavine, K.,
576 Mittal, V., May, B., Kasschau, K.D., Carrington, J.C., Doerge, R.W., Colot, V., Martienssen,
577 R. (2004) Role of transposable elements in heterochromatin and epigenetic control. *Nature*,
578 **430**(6998), 471-476.
- 579 Loake, G. and Grant, M. (2007) Salicylic acid in plant defence--the players and protagonists. *Current*
580 *Opinion in Plant Biology*, **10**(5), 466-472.

- 581 Lodhi, N., Ranjan, A., Singh, M., Srivastava, R., Singh, S.P., Chaturvedi, C.P., Ansari, S.A., Sawant,
582 S.V., Tuli, R. (2008) Interactions between upstream and core promoter sequences determine
583 gene expression and nucleosome positioning in tobacco PR-1a promoter. *Biochimica et*
584 *Biophysica Acta (BBA) - Gene Regulatory Mechanisms*, **1779**(10), 634-644.
- 585 Lomvardas, S. and Thanos, D. (2001) Nucleosome sliding via TBP DNA binding in vivo. *Cell*,
586 **106**(6), 685-696.
- 587 Lomvardas, S. and Thanos, D. (2002) Modifying gene expression programs by altering core promoter
588 chromatin architecture. *Cell*, **110**(2), 261-271.
- 589 Mathieu, O., Probst, A.V., Paszkowski, J. (2005) Distinct regulation of histone H3 methylation at
590 lysines 27 and 9 by CpG methylation in Arabidopsis. *The EMBO Journal*, **24**(15), 2783-2791.
- 591 Metzger, E., Wissmann, M., Yin, N., Muller, J.M., Schneider, R., Peters, A.H., Gunther, T., Buettnner,
592 R., Schule, R. (2005) LSD1 demethylates repressive histone marks to promote androgen-
593 receptor-dependent transcription. *Nature*, **437**(7057), 436-439.
- 594 Mosher, R.A., Durrant, W.E., Wang, D., Song, J., Dong, X. (2006) A comprehensive structure-
595 function analysis of Arabidopsis SNI1 defines essential regions and transcriptional repressor
596 activity. *The Plant Cell*, **18**(7), 1750-1765.
- 597 Naumann, K., Fischer, A., Hofmann, I., Krauss, V., Phalke, S., Irmeler, K., Hause, G., Aurich, A.C.,
598 Dorn, R., Jenuwein, T., Reuter, G. (2005) Pivotal role of AtSUVH2 in heterochromatic
599 histone methylation and gene silencing in Arabidopsis. *The EMBO Journal*, **24**(7), 1418-
600 1429.
- 601 Nishioka, K., Rice, J.C., Sarma, K., Erdjument-Bromage, H., Werner, J., Wang, Y., Chuikov, S.,
602 Valenzuela, P., Tempst, P., Steward, R., Lis, J.T., Allis, C.D., Reinberg, D. (2002) PR-Set7 is
603 a nucleosome-specific methyltransferase that modifies lysine 20 of histone H4 and is
604 associated with silent chromatin. *Molecular Cell*, **9**(6), 1201-1213.
- 605 Santos-Rosa, H. and Caldas, C. (2005) Chromatin modifier enzymes, the histone code and cancer.
606 *European Journal of Cancer*, **41**(16), 2381-2402.
- 607 Sarg, B., Helliger, W., Talasz, H., Koutzamani, E., Lindner, H.H. (2004) Histone H4 hyperacetylation
608 precludes histone H4 lysine 20 trimethylation. *Journal of Biological Chemistry*, **279**(51),
609 53458-53464.
- 610 Shahbazian, M.D. and Grunstein, M. (2007) Functions of site-specific histone acetylation and
611 deacetylation. *Annual Review of Biochemistry*, **76**, 75-100.
- 612 Shogren-Knaak, M. and Peterson, C.L. (2006) Switching on chromatin: mechanistic role of histone
613 H4-K16 acetylation. *Cell Cycle*, **5**(13), 1361-1365.
- 614 Sims, R.J., 3rd, Nishioka, K., Reinberg, D. (2003) Histone lysine methylation: a signature for
615 chromatin function. *Trends in Genetics*, **19**(11), 629-639.
- 616 Spoel, S.H., Koornneef, A., Claessens, S.M., Korzelius, J.P., Van Pelt, J.A., Mueller, M.J., Buchala,
617 A.J., Métraux, J.P., Brown, R., Kazan, K., Van Loon, L.C., Dong, X., Pieterse, C.M. (2003)
618 NPR1 modulates cross-talk between salicylate- and jasmonate-dependent defense pathways
619 through a novel function in the cytosol. *The Plant Cell*, **15**(3), 760-770.
- 620 Srivastava, R. and Ahn, S.H. (2015) Modifications of RNA polymerase II CTD: Connections to the
621 histone code and cellular function. *Biotechnology Advances*, **33**(6, Part 1), 856-872.
- 622 Srivastava, R., Rai, K.M., Srivastava, M., Kumar, V., Pandey, B., Singh, S.P., Bag, S.K., Singh, B.D.,
623 Tuli, R., Sawant, S.V. (2014) Distinct Role of Core Promoter Architecture in Regulation of
624 Light-Mediated Responses in Plant Genes. *Molecular Plant*, **7**(4), 626-641.
- 625 Srivastava, R., Singh, U.M., Dubey, N.K. (2016) Histone Modifications by different histone
626 modifiers: insights into histone writers and erasers during chromatin modification. *Journal of*
627 *Biological Sciences and Medicine*, **2**(1), 45-54.
- 628 Struhl, K. (1998) Histone acetylation and transcriptional regulatory mechanisms. *Genes &*
629 *Development*, **12**(5), 599-606.
- 630 Sung, S. and Amasino, R.M. (2004) Vernalization and epigenetics: how plants remember winter.
631 *Current Opinion in Plant Biology*, **7**(1), 4-10.
- 632 Tsuji, H., Saika, H., Tsutsumi, N., Hirai, A., Nakazono, M. (2006) Dynamic and reversible changes in
633 histone H3-Lys4 methylation and H3 acetylation occurring at submergence-inducible genes in
634 rice. *Plant and Cell Physiology*, **47**(7), 995-1003.

- 635 Tsukada, Y., Fang, J., Erdjument-Bromage, H., Warren, M.E., Borchers, C.H., Tempst, P., Zhang, Y.
636 (2006) Histone demethylation by a family of JmjC domain-containing proteins. *Nature*,
637 **439**(7078), 811-816.
- 638 Turck, F., Roudier, F., Farrona, S., Martin-Magniette, M.L., Guillaume, E., Buisine, N., Gagnot, S.,
639 Martienssen, R.A., Coupland, G., Colot, V. (2007) Arabidopsis TFL2/LHP1 specifically
640 associates with genes marked by trimethylation of histone H3 lysine 27. *PLOS Genetics*, **3**(6),
641 e86.
- 642 Turner, B.M. (2000) Histone acetylation and an epigenetic code. *Bioessays*, **22**(9), 836-845.
- 643 Vlot, A.C., Dempsey, D.A., Klessig, D.F. (2009) Salicylic Acid, a multifaceted hormone to combat
644 disease. *Annual Review of Phytopathology*, **47**, 177-206.
- 645 Wang, X., Basnayake, B.M., Zhang, H., Li, G., Li, W., Virk, N., Mengiste, T., Song, F. (2009) The
646 Arabidopsis ATAF1, a NAC transcription factor, is a negative regulator of defense responses
647 against necrotrophic fungal and bacterial pathogens. *Molecular Plant-Microbe Interactions*,
648 **22**(10), 1227-1238.
- 649 Whetstine, J.R., Nottke, A., Lan, F., Huarte, M., Smolikov, S., Chen, Z., Spooner, E., Li, E., Zhang,
650 G., Colaiacovo, M., Shi, Y. (2006) Reversal of histone lysine trimethylation by the JMJD2
651 family of histone demethylases. *Cell*, **125**(3), 467-481.
- 652 Workman, J.L. and Kingston, R.E. (1998) Alteration of nucleosome structure as a mechanism of
653 transcriptional regulation. *Annual Review of Biochemistry*, **67**, 545-579.
- 654 Yamane, K., Toumazou, C., Tsukada, Y., Erdjument-Bromage, H., Tempst, P., Wong, J., Zhang, Y.
655 (2006) JHDM2A, a JmjC-containing H3K9 demethylase, facilitates transcription activation
656 by androgen receptor. *Cell*, **125**(3), 483-495.
- 657 Zhang, X., Bernatavichute, Y.V., Cokus, S., Pellegrini, M., Jacobsen, S.E. (2009) Genome-wide
658 analysis of mono-, di- and trimethylation of histone H3 lysine 4 in Arabidopsis thaliana.
659 *Genome Biology*, **10**(6), R62.
- 660 Zhou, C., Zhang, L., Duan, J., Miki, B., Wu, K. (2005) HISTONE DEACETYLASE19 is involved in
661 jasmonic acid and ethylene signaling of pathogen response in Arabidopsis. *The Plant Cell*,
662 **17**(4), 1196-1204.
- 663

664 **FIGURE LEGENDS**

665 **Fig. 1. Mapping border sequences of the core nucleosome.**

666 (A) Lane 1: Amplified product of reverse primer (NR1). Lane 2: Amplified product of
667 forward primer (PF3). Lane 3 and 4: non template controls for NR1 and PF3 (negative
668 controls). Lanes 5 to 8: sequence ladders for T, G, C and A respectively. (B)
669 Nucleotide sequence of core promoter of tobacco *PR-1a* promoter showing in bold the
670 -102 to +55 region covered by the nucleosome. The TATA, *Inr* like region and
671 downstream promoter like sequences are underlined and TSS is showed by arrow.

672 **Fig. 2. Time course analysis of the acetylation chromatin state on the tobacco *PR-1a* 673 core promoter region in uninduced and induced state, and *AtPR1* expression in 674 Arabidopsis HAT mutants.**

675 (A) Histone acetylation status on R8 was analyzed by ChIP assay using A) anti-acetyl
676 H3K9, B) anti-acetyl H4K16 antibodies. The immunoprecipitated DNA was analyzed
677 by qRT-PCR. The histogram represents the % input (Y-axis) at different time points
678 (X-axis) with SD. Constitutive expression of *AtPR1* in HAG3, HAC1, HXA1 gene

679 mutant lines of *Arabidopsis* in comparison to wild type (Ws) in uninduced state and
680 quantitative (C). *AtPR1* expression was quantified by real-time PCR.

681 **Fig. 3. Nucleosome mapping on the *PR-1a* core promoter region in uninduced, SA, TSA**
682 **and SA + TSA treated leaves by anti-H3 ChIP- PCR.**

683 (A) Standard PCR was done to detect nucleosomes in the core promoter (-102 to +55
684 bp) and flanking upstream (-102 to -213 bp and -213 to -362 bp) and downstream
685 (+59 to +319 bp) regions of the native *PR-1a* promoter. The Input DNA is used as
686 ChIP control (for each primer set) as shown below each lane. (B) The models depict
687 the location of nucleosomes on *PR-1a* promoter before and after SA induction upon
688 the regions analyzed in (A).

689 **Fig. 4. Temporal changes in histone acetylation at *PR-1a* core promoter in relation to**
690 ***PR-1a* transcript.**

691 The ChIP assay was performed on tobacco leaves floated on SA for 3 to 18 h, using
692 antibodies against acetylated H3K9/14. The PCR products from immunoprecipitated
693 DNA (correspond to core promoter region) are shown at different time points. The
694 input template was used as control. Tobacco *PR-1a* transcripts were estimated by RT-
695 PCR at different time points, following SA induction. Tobacco *UBQ* was used as an
696 internal control for transcript analysis.

697 **Fig. 5. Effect of TSA on tobacco *PR-1a* expression, following induction with SA.**

698 Leaf discs from the *PR-1a*:GUS transgenic tobacco were placed in 2 mM SA for 4h
699 only then were shifted to water or TSA for different time intervals, as indicated. The
700 GUS assay was performed after 24 h of time completion. The kinetics of GUS
701 expression *PR-1a* in the presence of water (▲) and TSA (■) is shown in Fig..

702 **Fig. 6. Time course analysis of the methylation status on R8 upon SA induction for**
703 **different time periods.**

704 Histone methylation status on R8 was analyzed by ChIP assay using antibodies
705 against mono-, di- and tri-methyl H3-K4, H3-K9 and H4-K20 (A-I). ChIP assay was
706 performed using these antibodies on tobacco leaves treated with water (uninduced) or
707 SA (induced) up to 24 h. The immunoprecipitated DNA was analyzed by qRT-PCR.
708 The histogram represents the % input (Y-axis) at different time points (X-axis) with
709 SD.

710 **Fig. 7. Expression of *AtPR1* in mutant plants of *Arabidopsis* and ChIP- PCR analysis**
711 **using anti-LSD1, anti- CoREST and anti-HDAC1 antibodies at *PR-1a* promoter**
712 **locus.** Constitutive expression of *AtPR1* in gene mutant lines of *A. thaliana* in

713 comparison to wild type in uninduced state. **(A)**. *AtPRI* expression in four LSD1 like
714 gene mutant lines was quantified by qRT-PCR. **(B)**. Expression of *AtPRI*, *AtSNII*,
715 *AtPDF1.2* and *AtGDAS* transcripts in *Arabidopsis*. Transcript levels were estimated
716 by RT-PCR, 24 h after floating the leaves on water, SA, TSA and SA +TSA. The
717 *AtACTIN7* was used as an internal control. **(C)**. Presence of LSD1 on chromatin of
718 core promoter region of *PR-1a* was analysed by ChIP assay using anti-LSD1
719 antibody. The immunoprecipitated DNA was analyzed by standard PCR. Input DNA
720 was used as ChIP control. **(D)**. Detection of LSD1-like complex at core promoter
721 region of *PR-1a* in uninduced state by ChIP PCR. ChIP assay was performed by using
722 antibodies against LSD1, CoREST and HDAC1. The representative PCR products
723 indicate the presence of LSD1, CoREST and HDAC1, in uninduced state. Input DNA
724 was used as ChIP control.

725 **Fig. 8. Probable Model suggesting the sequential events and ordered modifications of**
726 **chromatin over the *PR-1a* promoter in tobacco leaf.**

727 Histone modifications associated with various *PR-1a* promoter states are shown. The
728 promoter region has six distinct nucleosomes including downstream nucleosome in
729 the repressed state, as shown in **(A)**. The nucleosome over core promoter has
730 repressive histone marks (mono, di and trimethylated H4-K20 and H3-K9) and LSD1-
731 CoREST-HDAC1 repressor complex **(A)**. Following SA mediated activation **(B)** of
732 *PR-1a* promoter, the repressor complex is dissociated from the core promoter region,
733 possibly through the recruitment of histone acetyltransferase, resulting in H3K9ac and
734 H4K16ac. Active histone methylation marks (mono, di and trimethylated H3-K4) also
735 increase. Acetylation at H3-K9/14 and H4-K12 lead to decrease in histone–DNA
736 interactions eventually nucleosome disappears from the core promoter **(C)** region,
737 leading to the recruitment of pre-initiation complex (PIC). The new incorporated
738 histone codes (mono, di and trimethylation of H3-K4, and acetylation of H3-K9/14
739 and H4-K12) make actively transcribed *PR-1a* chromatin.

Fig. 1

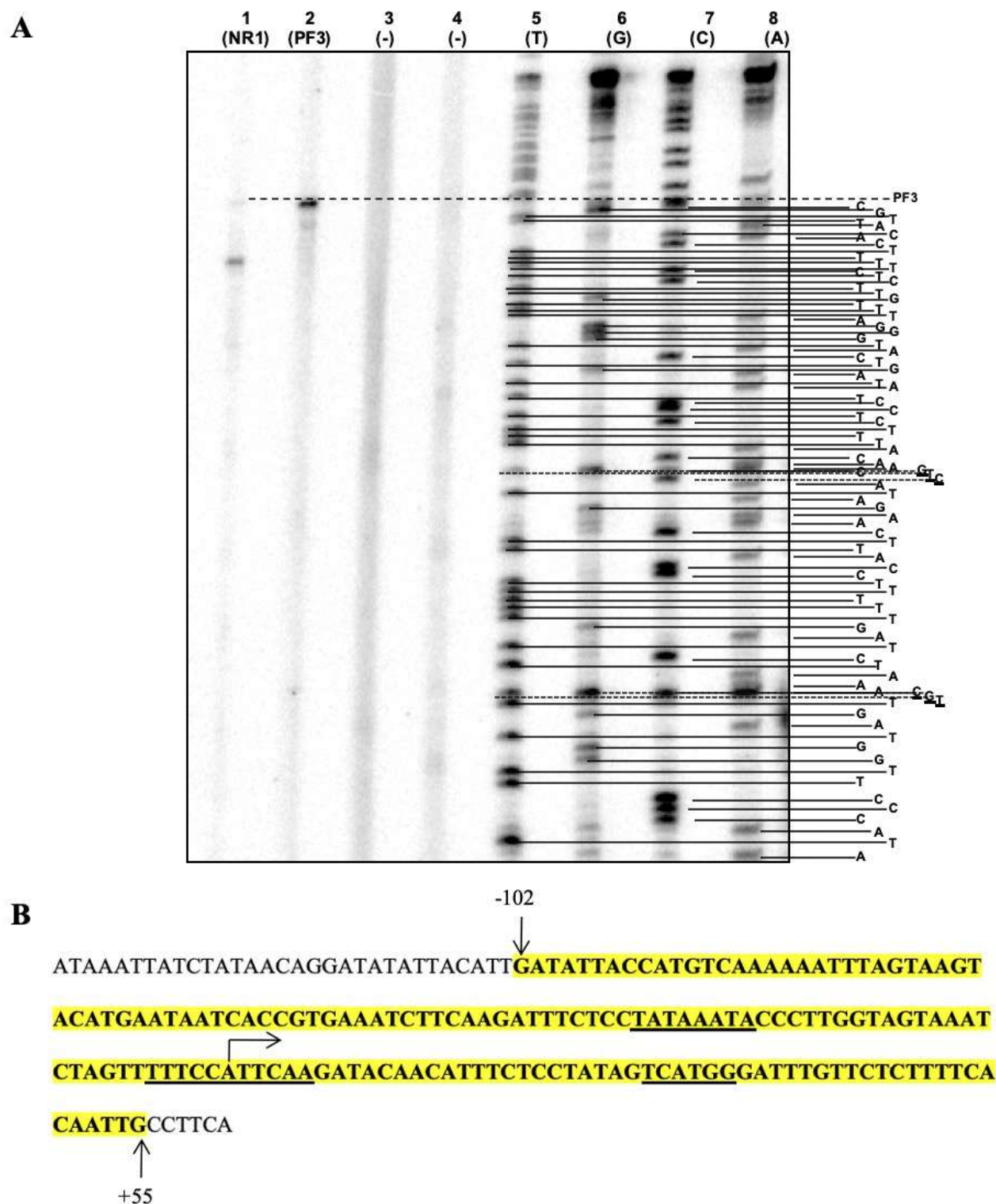


Figure 1: Mapping of borders sequences of the core nucleosome by primer extension.

(A) Lane 1: Amplified product of reverse primer (NR1). Lane 2: Amplified product of forward primer (PF3). Lane 3 and 4: non template controls for NR1 and PF3 (negative controls). Lanes 5 to 8: sequence ladders for T, G, C and A respectively. (B) Nucleotide sequence of core promoter of tobacco *PR-1a* promoter showing in dark and shadowed the -102 to +55 region covered by the nucleosome. The TATA, *Inr* like region and downstream promoter like sequences are underlined. The transcription start site is shown by arrow.

Fig. 2

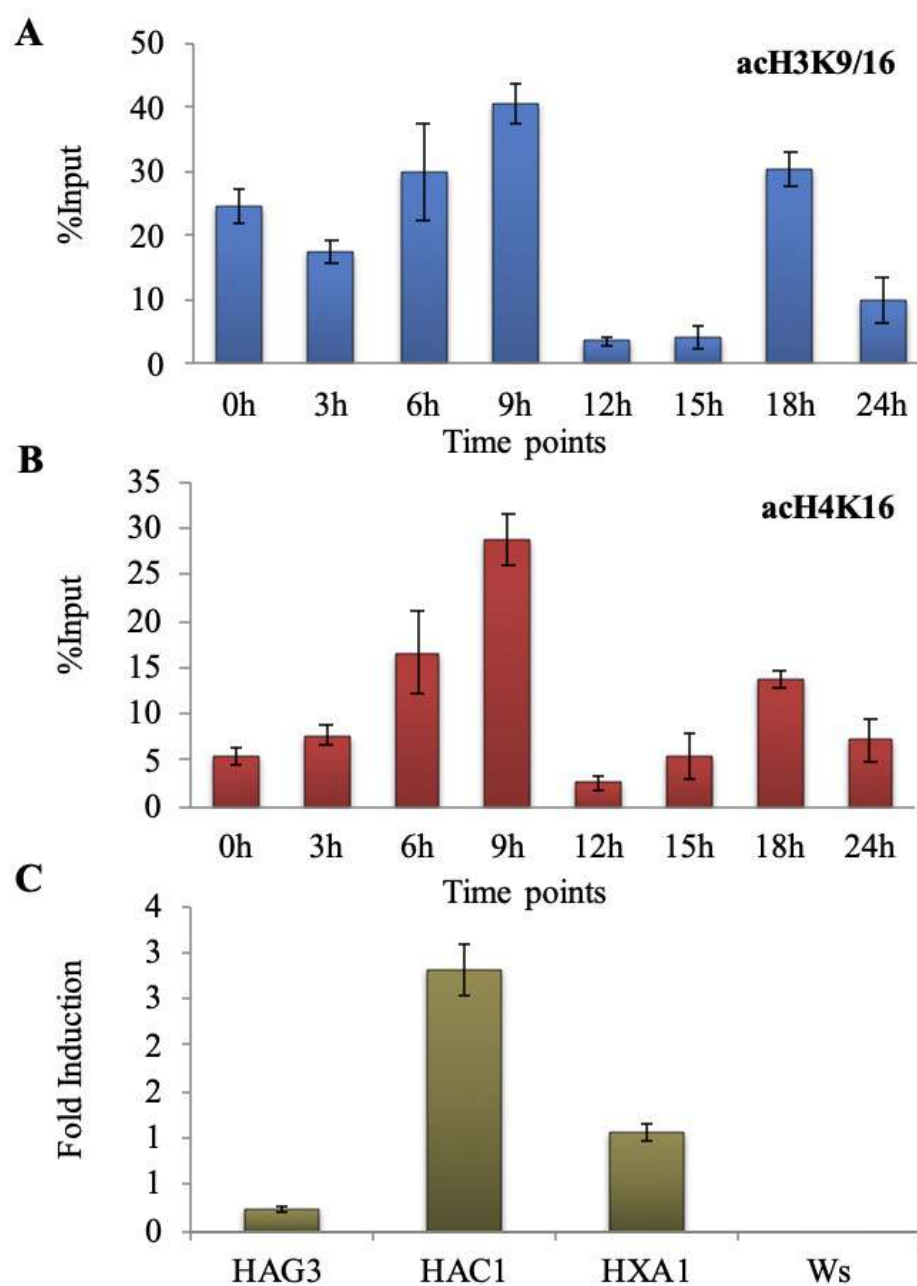


Figure 2: Time course analysis of the acetylation chromatin state on core promoter region of tobacco *PR-1a* in uninduced and induced state and the expression of *AtPR1* in HAT mutants of *Arabidopsis*.

Histone acetylation status on R8 was analyzed by ChIP assay using (A) anti-acetyl H3K9, (B) anti-acetyl H4K16 antibodies. The immunoprecipitated DNA was analyzed by qPCR. The histogram represents the % input (Y-axis) at different time points (X-axis) with SD. Constitutive expression of *AtPR1* in HAG3, HAC1, HXA1 gene mutant lines of *Arabidopsis* in comparison to wild type (Ws) in uninduced state and quantitative (C). *AtPR1* expression was quantified by real-time PCR.

Fig. 3

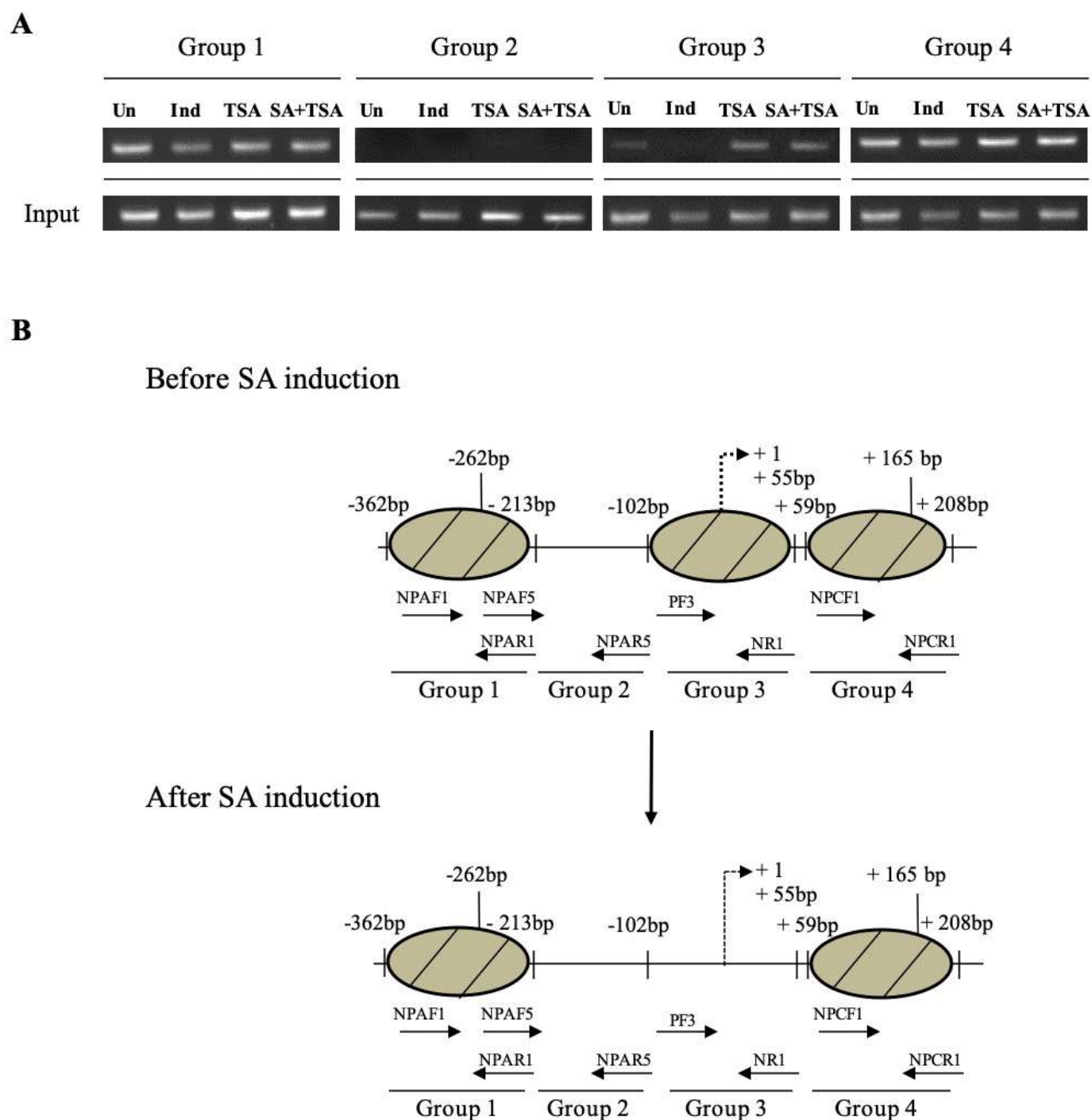


Figure 3: Nucleosome mapping on core promoter region of the *PR-1a* promoter in uninduced, SA, TSA and SA+TSA treated leaves by anti-H3 ChIP-PCR.

(A) Standard PCR was done to detect nucleosomes in the core promoter (-102 to +55 bp) and flanking upstream (-102 to -213 bp and -213 to -362 bp) and downstream (+59 to +319 bp) regions of the native *PR-1a* promoter. The Input DNA is used as ChIP control (for each primer set) as shown below each lane. (B) The models depict the location of nucleosomes on *PR-1a* promoter before and after SA induction upon the regions analysed.

Fig. 4

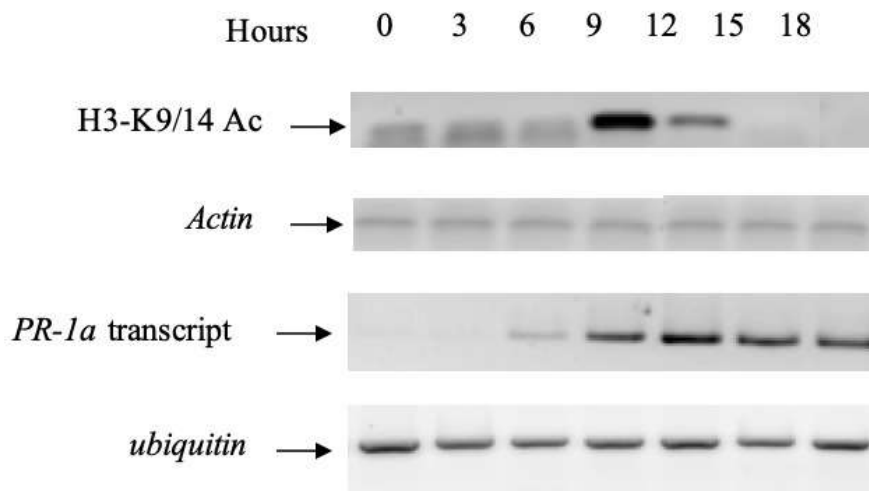


Figure 4: Temporal changes in histone acetylation at *PR-1a* core promoter in relation to *PR-1a* transcript.

The ChIP assay was performed on tobacco leaves floated on SA for 3 to 18 h, using antibodies against acetylated H3K9/14 and tri-methylation of H3K4. The PCR products from immunoprecipitated DNA (correspond to core promoter region) are shown at different time points. The input template was used as control. Tobacco *PR-1a* transcripts were estimated by RT-PCR at different time points, following SA induction. Tobacco *UBQ* was used as an internal transcript control for transcript analysis.

Fig. 5

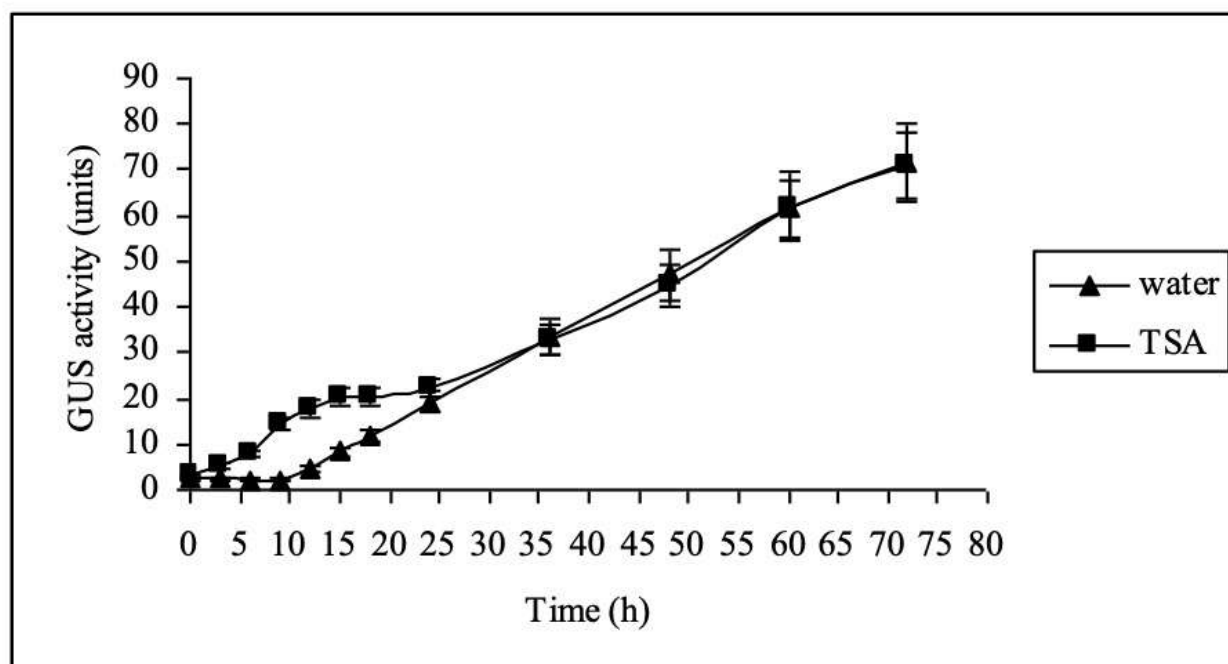


Figure 5: Effect of TSA on tobacco *PR-1a* expression, following induction with SA.

Leaf discs from the *PR-1a*:GUS transgenic tobacco were placed in 2 mM SA for 4h only then were shifted to water or TSA for different time intervals, as indicated. The GUS assay was performed after 24 h of time completion. The kinetics of GUS expression *PR-1a* in the presence of water (▲) and TSA (■) is shown in figure.

Fig. 6

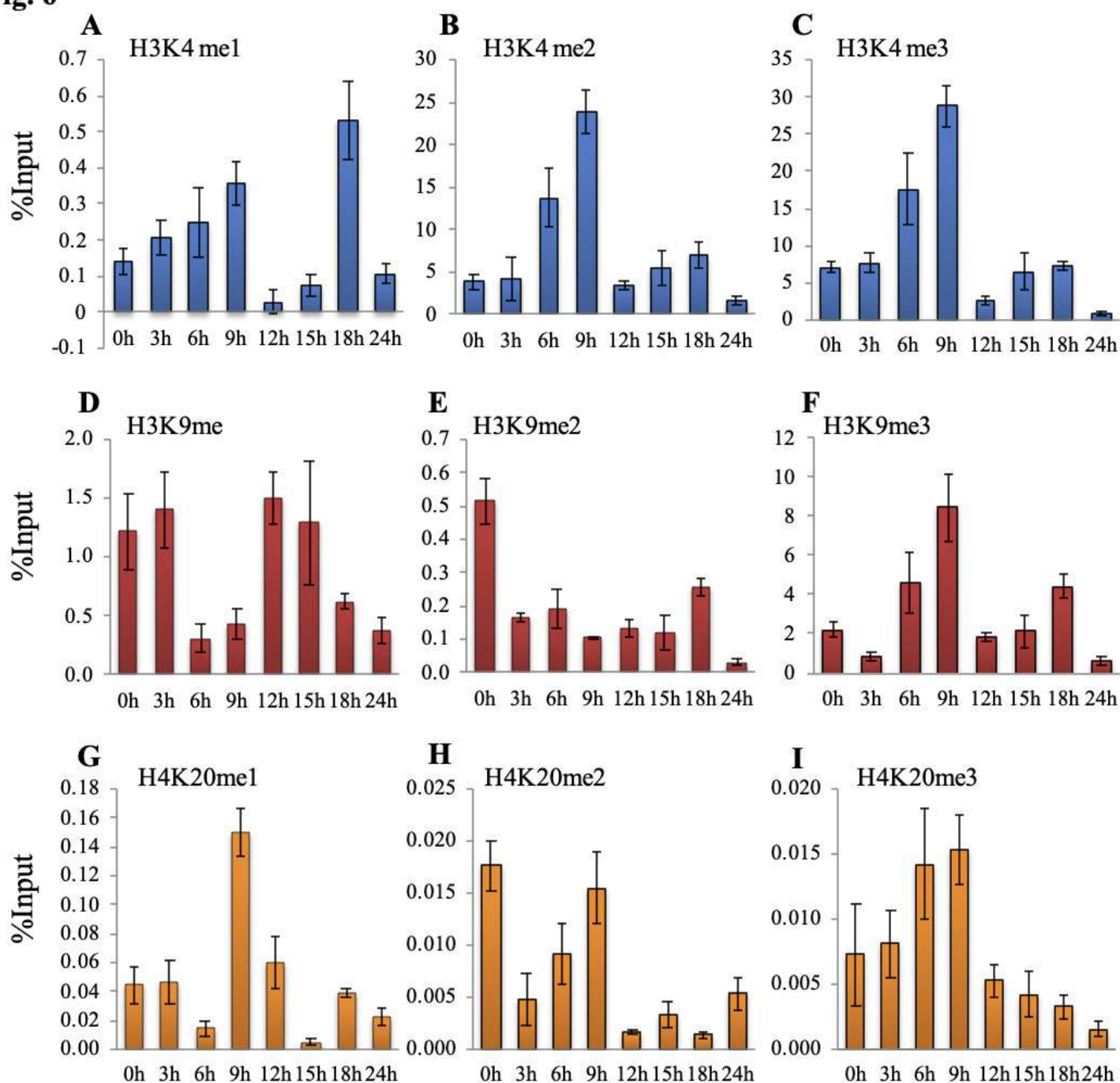


Figure 6: Histone methylation status of chromatin on core promoter region of tobacco *PR-1a* promoter in uninduced and induced state.

Histone methylation status on R8 was analyzed by ChIP assay using antibodies against mono-, di- and tri-methyl H3-K4, H3-K9 and H4-K20 (A-I). ChIP assay was performed using these antibodies on tobacco leaves treated with water (uninduced) or SA (induced) up to 24 h. The immunoprecipitated DNA was analyzed by qPCR. The histogram represents the % input (Y-axis) at different time points (X-axis) with SD.

Fig. 7

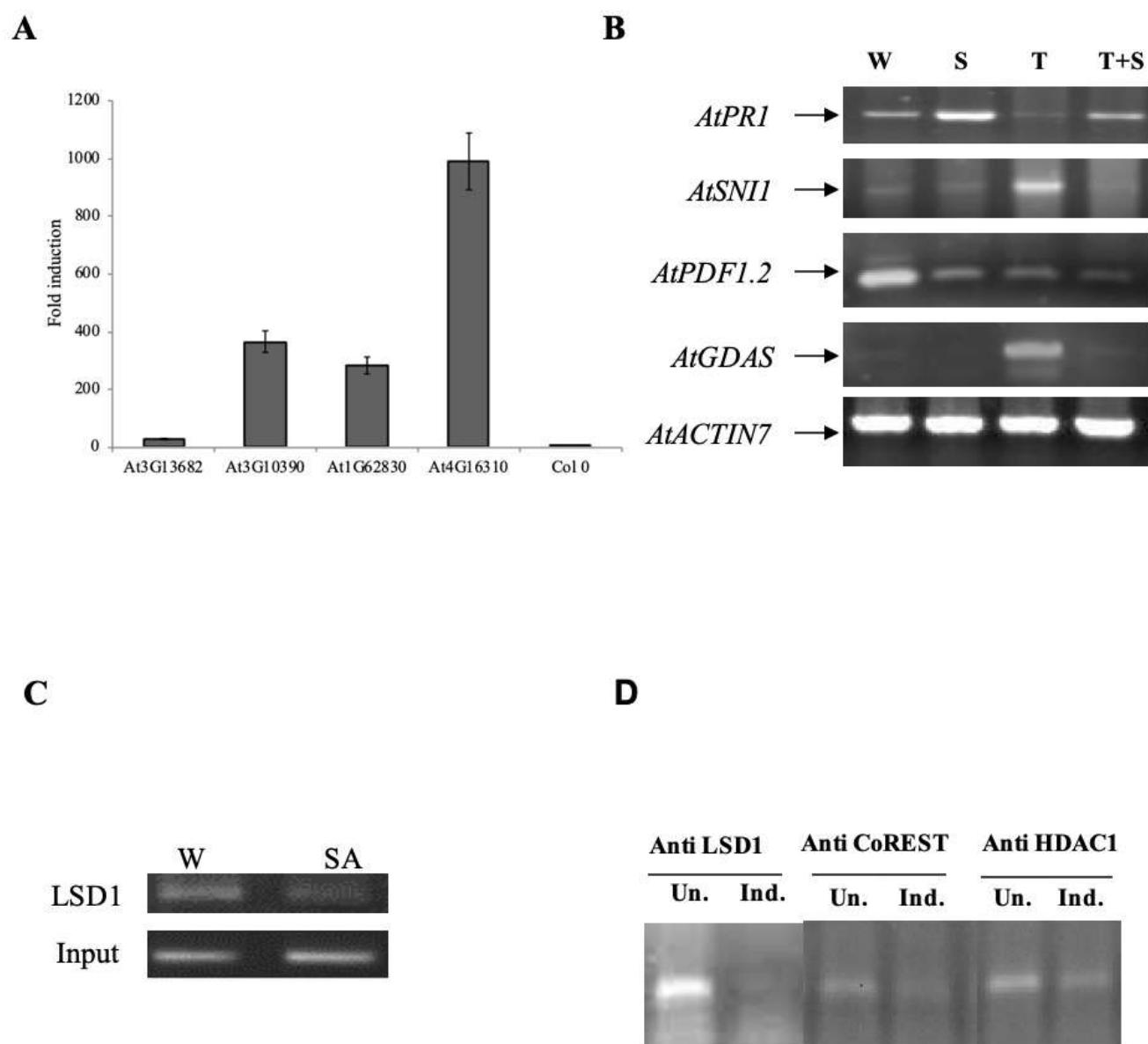


Figure 7: Expression of *AtPR1* in mutant plants of *Arabidopsis*.

(A) Constitutive expression of *AtPR1* in four different LSD1 like gene mutant lines of *A. thaliana* in comparison to wild type in uninduced state. *AtPR1* expression was quantified by real-time PCR.

(B) ChIP- PCR analysis using anti-LSD1 antibody at *PR-1a* promoter locus. Presence of LSD1 on chromatin of core promoter region of *PR-1a* was analysed by ChIP assay using anti-LSD1 antibody. The immunoprecipitated DNA was analyzed by standard PCR. Input DNA was used as ChIP control.

Fig. 8

